Journal of Alloys and Compounds 517 (2012) 111–117

Contents lists available at SciVerse ScienceDirect

Journal of Alloys and Compounds

journal homepage: www.elsevier.com/locate/jallcom

Interfacial reactions of Pb-free solders with Au/Pd/Ni/brass multilayer substrates

Yee-wen Yen[a,*], Po-hao Tsai[b], Yang-kai Fang[b], Bo-jyun Chen[a], Chiapyng Lee[b]

[a] Department of Material Science and Engineering, National Taiwan University of Science and Technology, Taipei 106, Taiwan, ROC
[b] Department of Chemical Engineering, National Taiwan University of Science and Technology, Taipei 106, Taiwan, ROC

ARTICLE INFO

Article history:
Received 6 September 2011
Received in revised form 7 December 2011
Accepted 12 December 2011
Available online 19 December 2011

Keywords:
Interfacial reaction
Lead-free solder
Au/Pd/Ni/brass multilayer substrate
Intermetallic compound

ABSTRACT

The interfacial reactions of Sn, Sn–3.0 wt% Ag–0.5 wt% Cu (SAC), Sn–0.7 wt% Cu (SC), Sn–58 wt% Bi (SB) and Sn–9 wt% Zn (SZ) lead-free solders with an Au/Pd/Ni/brass multilayer substrate were systematically investigated in this study. The results revealed that $(Cu, Ni)_6Sn_5$ and CuZn phases were formed at the interface in the Sn, SAC, and SC solders reacting with Au/Pd/Ni/brass systems. In the SB/Au/Pd/Ni/brass system, $(Ni, Cu)_3Sn_4$, $(Cu, Ni)_6Sn_5$ and CuZn phases were formed at the interface. The $CuZn_5$, Pd_2Zn_9, Ni_5Zn_{21} and Cu_5Zn_8 phases were formed in the SZ/Au/Pd/Ni/brass system.

1. Introduction

As computer, communication and consumer (3C) electronic products have become lighter, thinner and smaller, these devices require increased high in/out (IO) connecting density and reliable solders. Thus, flip chip (FC) and ball grid array (BGA) techniques have dominated connecting techniques due to their high interconnection density. The demand for improved solders is greater than before. In the past Sn–Pb solders were widely used in soldering processes due to their excellent soldering characteristics and reliability [1,2]. However, Pb is a heavy metal that reacts with acidic rain to form the lead carbonate, which is harmful to human health [3]. Two important laws, such as the waste from electrical and electronic equipment (WEEE) and restriction of hazardous substances directive (RoHs) which were legislated by the European Union (EU), forbid the sale of Pb-containing 3C products since July 1, 2007 [4]. Several Pb-free solders, such as Sn, Sn–3.0 wt% Ag–0.5 wt% Cu (SAC), Sn–0.7 wt% Cu (SC), Sn–58.0 wt% Bi (SB) and Sn–9.0 wt% Zn (SZ) have replaced Sn–Pb solders today [5–14].

A brass is a Cu–Zn alloy. The Zn content in the brass is usually 5–40 wt%. The brass has better mechanical properties, fine brightness, suitable workability and good corrosion resistance compared to a pure Cu. The brass is therefore one of the most popular substrates used in the electronics industry. An Au/Pd/Ni multilayer structure is commonly electroplated onto a metallic substrate surface to improve the joint reliability and wettability between the solder and substrate. Numerous studies have reported on the interfacial reactions of Pb-free solders with Au/Pd/Ni/metallic substrates [14–26]. However, research on the interfacial reactions between the solder and Au/Pd/Ni/brass systems is lacking. Only one reference regarding the Sn–Zn–Bi solder reacting with a brass substrate could be found [27]. Because the brass is a popular substrate material, it is necessary to clearly understand the interfacial reactions between lead-free solders and brass. This study uses the liquid/solder reaction couple technique to investigate the interfacial reactions of the Au/Pd/Ni/brass multilayer substrate in molten Sn, SAC, SB and SZ Pb-free solders at 240, 255 and 270 °C for various reaction time periods.

2. Experimental

The brass substrate (Cu–40 wt% Zn alloy) was electroplated with a 75 nm-thick Au layer, 210 nm-thick Pd layer, and 1.78 μm-thick Ni layer, respectively. This multilayer substrate was provided by Hon Hai Precision Ind. Co., Ltd. The Au/Pd/Ni/brass multilayer substrate with 15.0 (length) × 5.0 (width) × 1.0 (thickness) mm was ultrasonically cleaned in ethanol and de-ionized water to ensure that there were no contaminates on the substrate surface. The Sn, Sn–3.0 wt% Ag–0.5 wt% Cu (SAC), Sn–0.7 wt% Cu (SC), Sn–58.0 wt% Bi (SB) solders are commercial solders. The Sn–9.0 wt% Zn (SZ) solder was prepared with Sn and Zn shots above 99.0 wt% purity. The SZ solder with a total mass of 2.0 g was encapsulated in a quartz tube in a 0.1 N/m^2 vacuum. The sample tube was first placed in a furnace at 500 °C for 48 h to ensure a homogeneous liquid mixing of the constituent elements and then quenched in ice water. The liquid/solid reaction couples were prepared in this study. The cleaned Au/Pd/Ni/brass multilayer substrate was dipped in rosin mildly activated (RMA) flux and reacted with these solders in an evacuated quartz tube. The substrate/solder mass ratio was about 1/3. The couples were placed in a tube furnace at 240, 255 and 270 °C for 20 min and 1, 2, 4, 8, 20 h.

After the solid/liquid interfacial reactions, all couples were subsequently quenched in ice water. The sample was first examined metallurgically. The reaction couples were mounted in an epoxy resin and ground polished carefully to

* Corresponding author. Tel.: +886 2 27376659; fax: +886 2 27301265.
E-mail address: ywyen@mail.ntust.edu.tw (Y.-w. Yen).

0925-8388/$ – see front matter © 2011 Elsevier B.V. All rights reserved.
doi:10.1016/j.jallcom.2011.12.046

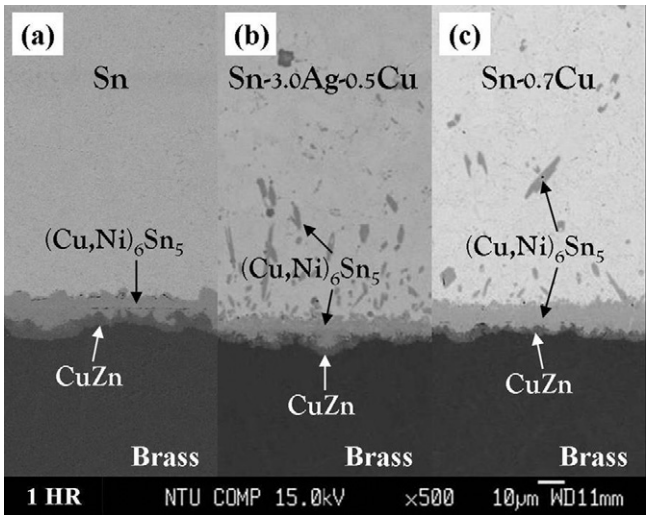

Fig. 1. BEI micrographs of the (a) Sn/Au/Pd/Ni/brass, (b) SAC/Au/Pd/Ni/brass and (c) SC/Au/Pd/Ni/brass reaction systems reacted at 270 °C for 1 h.

make the cross-sectional interface perpendicular to the exposed substrates. An optical microscope (OM) and scanning electron microscope (SEM) were used for the microstructure examination. If intermetallic compounds (IMCs) were formed at the interface, a SEM with an energy dispersive spectrometer (EDS) and electron probe micro-analyzer (EPMA) were used to determine the IMC composition. This result was compared with the related phase diagrams to identify the IMC. A deep-etching technique was employed to remove the solder to observe a three-dimensional (3-D) IMC microstructure. The detailed etching solution compositions for each solder/substrate couple are listed in a previous study [14].

3. Results and discussion

3.1. Sn/Au/Pd/Ni/brass reaction couple

Fig. 1(a) shows a backscatter electron image (BEI) of the Sn solder reacting with the Au/Pd/Ni/brass substrate at 270 °C for 1 h. Two different contrast layers are observed at the interface. Similar to the Sn/Au/Pd/Ni/Cu system [14], the Au and Pd layers are completely dissolved into the molten Sn. Meanwhile, the Cu atoms from the brass also dissolved into the molten Sn. Thus, the (Cu, Ni)$_6$Sn$_5$ phase of Sn–28.0 Cu–22.0 Ni–5.0 Zn (at.%) was formed close to the Sn side [28]. Because the Au and Pd layers are thin enough, the Au and Pd concentrations were too limited to detect. That's why no Pd or Au atoms were found in the (Cu, Ni)$_6$Sn$_5$ phase. The brass is a Cu–40 wt% Zn alloy. When Cu atoms dissolve toward molten Sn, the Zn concentration becomes greater than 40 wt%, forming stable Cu–Zn phases. Thus, the CuZn phase with a Cu–46.6 Zn–6.3 Sn (at.%) composition was observed at the substrate side [28], as shown in Fig. 1(a).

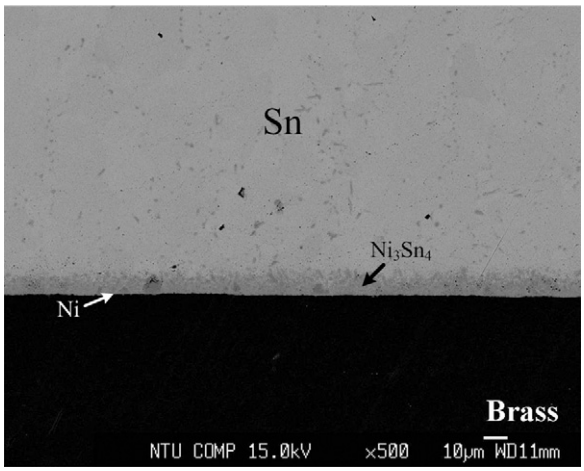

Fig. 3. BEI micrographs of the Sn/Au/Pd/Ni/brass reaction systems reacted at 240 °C for 20 min.

Due to the fact that the brass is a Cu–Zn alloy, the CuZn phase was formed at the interface. The reaction mechanism might be that the (Cu, Ni)$_6$Sn$_5$ phase acted as a diffusion barrier to prevent the Sn atoms from diffusing toward the brass and the Gibbs formation energy of the Cu–Zn IMCs was lower than that of the Cu–Sn IMCs [20]. The Cu and Zn atoms in the brass thus reacted with each other to form the CuZn phase at the interface. When compared with the previous study [14], the Cu$_3$Sn phase was not formed in the Au/Pd/Ni/brass system. The reason might be that the CuZn layer also acts as a diffusion barrier so that not enough Sn atoms could diffuse toward the substrate to react with Cu to form the Cu$_3$Sn phase.

When the reaction time was increased to 20 h, only the (Cu, Ni)$_6$Sn$_5$ and CuZn phases were formed at the interface. The (Cu, Ni)$_6$Sn$_5$ phase with a larger grain and the CuZn phase with a cobble shape were formed between the solder and brass, as shown in Fig. 2. When the reaction time was increased, the (Cu, Ni)$_6$Sn$_5$ phase with small grain would ripen each other to form a larger one to reduce the free energy. This result was similar to the interfacial reactions between the molten solder and solid Cu substrate [14,19,21,22]. When the reaction temperatures were reduced to 255 or 240 °C, the (Cu, Ni)$_6$Sn$_5$ and CuZn phases were still formed at the interface. However, the Ni layer still remained at the interface and the Ni$_3$Sn$_4$ phase was formed at the interface in the Au/Pd/Ni/brass system reacted at 240 °C for 20 min, as shown in Fig. 3. The IMC evolution is listed in Table 1.

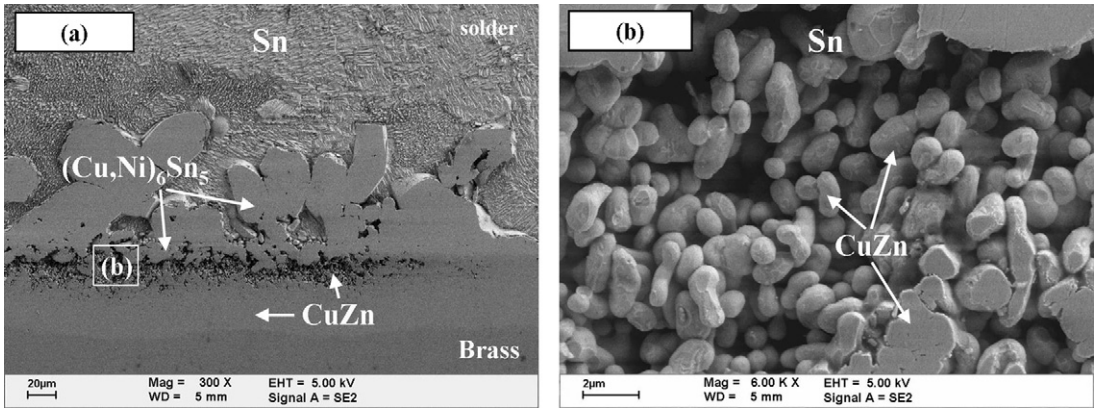

Fig. 2. (a) Deep-etched SEI microstructure of the Sn/Au/Pd/Ni/brass reaction system reacted at 270 °C for 20 h; (b) is magnified locally from (a).

Table 1
Summary of the IMCs formed in each solder/Au/Pd/Ni/brass systems.

Solder	Reaction temperature (°C)												
	240				250				270				
	Time												
	20 min	1–4 h	8 h	20 h	20 min	1–4 h	8 h	20 h	20 min	1–4 h	8 h	20 h	
Sn	Ni_3Sn_4	(Cu, $Ni)_6Sn_5$, CuZn			(Cu, $Ni)_6Sn_5$, CuZn				(Cu, $Ni)_6Sn_5$, CuZn				
SAC	(Cu, $Ni)_6Sn_5$	(Cu, $Ni)_6Sn_5$, CuZn			(Cu, $Ni)_6Sn_5$, CuZn				(Cu, $Ni)_6Sn_5$, CuZn				
SC	(Cu, $Ni)_6Sn_5$	(Cu, $Ni)_6Sn_5$, CuZn			(Cu, $Ni)_6Sn_5$	(Cu, $Ni)_6Sn_5$, CuZn			(Cu, $Ni)_6Sn_5$	(Cu, $Ni)_6Sn_5$, CuZn			
SB	Ni_3Sn_4		(Ni, $Cu)_3Sn_4$ (Cu, $Ni)_6Sn_5$ CuZn	(Cu, $Ni)_6Sn_5$ CuZn	Ni_3Sn_4		(Ni, $Cu)_3Sn_4$ (Cu, $Ni)_6Sn_5$ CuZn	(Cu, $Ni)_6Sn_5$ CuZn	Ni_3Sn_4		(Ni, $Cu)_3Sn_4$ (Cu, $Ni)_6Sn_5$ CuZn	(Cu, $Ni)_6Sn_5$ CuZn	
SZ	Pd_2Zn_9, Ni_5Zn_{21}			Pd_2Zn_9 Ni_5Zn_{21} Cu_5Zn_8	Pd_2Zn_9, Ni_5Zn_{21}			Pd_2Zn_9 Ni_5Zn_{21} Cu_5Zn_8	Pd_2Zn_9, Ni_5Zn_{21}				$CuZn_5$ Pd_2Zn_9 Ni_5Zn_{21} Cu_5Zn_8

SAC: Sn–3.0 wt% Ag–0.5 wt% Cu; SC: Sn–0.7 wt% Cu; SB: Sn–58 wt% Bi; SZ: Sn–9 wt% Zn.

The reaction mechanism for the Sn/Au/Pd/Ni/brass system is that the Au, Pd and Ni atoms rapidly dissolve into the molten Sn. At lower reaction temperatures the Ni atoms react with Sn to form the Ni_3Sn_4 phase. However, the Cu diffusion rate in Sn is faster than the Ni diffusion rate in Sn [29]. The Ni atoms are rapidly replaced by Cu atoms from the brass, which results in a Cu_6Sn_5 phase formed at the Sn side due to high Cu-concentration at the molten Sn/brass interface [14]. The Ni atoms can incorporate with the sublattice of the Cu_6Sn_5 phase to form a (Cu, $Ni)_6Sn_5$ phase, owing to the 40 at.% Ni solid solubility in Cu at 270 °C. However, the remaining Zn atoms react with Cu from the brass substrate to form the CuZn phase at the interface.

3.2. Sn–3.0 Ag–0.5 Cu (SAC)/Au/Pd/Ni/brass reaction couple

Fig. 1(b) shows a backscatter electron image (BEI) micrograph of the SAC/Au/Pd/Ni/brass system reacted at 270 °C for 1 h. Two different contrast layers can be observed at the interface. A gray, irregular, thick region close to the SAC solder has a unique composition of Sn–27.8 Cu–22.9 Ni–3.8 Zn (at.%). Due to the same structure, face-centered cubic (FCC), of the Cu and Ni atoms, a considerably amount of Ni atoms are incorporated into the Cu sublattice of the Cu_6Sn_5 phase. Thus, this layer is likely the (Cu, $Ni)_6Sn_5$ phase [28]. Furthermore, the dark, continuous and thin region near the brass side has a composition of Cu–46.3 Zn–6.0 Sn–1.3 Ag (at.%), and it is likely the CuZn phase [28]. Compared to the Sn/Au/Pd/Ni/brass couple, a few (Cu, $Ni)_6Sn_5$ phases were formed in the SAC solder due to the molten SAC solder segregation when the SAC solder quenched in ice water.

When the reaction time was extended to 20 h, the IMCs formed at the interface were still (Cu, $Ni)_6Sn_5$ and CuZn phases. The partial (Cu, $Ni)_6Sn_5$ phase peeled off progressively toward the solder. There was an obvious grain ripening phenomenon in the IMC at the interface when the reaction time was increased. This result is similar to that in the SAC/Au/Pd/Ni/Cu [14], SAC/Au/Ni/SUS 304 [24], and Sn–Ag–Cu/Ni [17] couples. Again, the Cu_3Sn phase was not formed at the interface. Because the Zn content is high at the solder/brass interface, the high activity Zn atoms would react with the Cu atoms from a SAC solder or brass to form a CuZn phase between the (Cu, $Ni)_6Sn_5$ and brass. Thus, the CuZn phase replaced the Cu_3Sn phase formed at the (Cu, $Ni)_6Sn_5$/brass interface.

Fig. 4(a) shows a deep-etched secondary electron image (SEI) micrograph of the SAC/Au/Pd/Ni/brass couple reacted at 270 °C for 8 h. There are massive IMCs peeled off from the interface found in Fig. 4. Fig. 4(b) and (c) is zoom-in images of Fig. 4(a). Similar to the SAC/Au/Pd/Ni/Cu couple, the (Cu, $Ni)_6Sn_5$ phases close to the SAC solder side, as shown in Fig. 4(b), have a polyhedron-type grain shape, owing to the great amount of Ni atoms dissolved in the (Cu, $Ni)_6Sn_5$ phase. Close to the CuZn phase, many small and spherical-type grains of the (Cu, $Ni)_6Sn_5$ phases having a lower Ni content were found in Fig. 4(a) and (c). According to the SC/Au/Ni/SUS 304 couple study [22], different Ni contents in the (Cu, $Ni)_6Sn_5$ phase indeed influences the grain morphology of the (Cu, $Ni)_6Sn_5$ phase. A great amount of Ag_3Sn particles with a small grain are adhered onto the (Cu, $Ni)_6Sn_5$ surface. Similar results were found when the reaction temperature was reduced to 250 and 240 °C. However, no CuZn phase was formed in the SAC/Au/Pd/Ni/brass system reacted at 240 °C only for 20 min. The IMC formation in this system is summarized in Table 1.

3.3. Sn–0.7 Cu (SC)/Au/Pd/Ni/brass reaction couple

Fig. 1(c) shows a BEI micrograph of the SC/Au/Pd/Ni/brass system reacted at 270 °C for 1 h. Two different layers could be found at the interface, as well. The composition of continuous and thin charcoal contrast layer near to the brass side is Cu–47.2 Zn–6.2 Sn

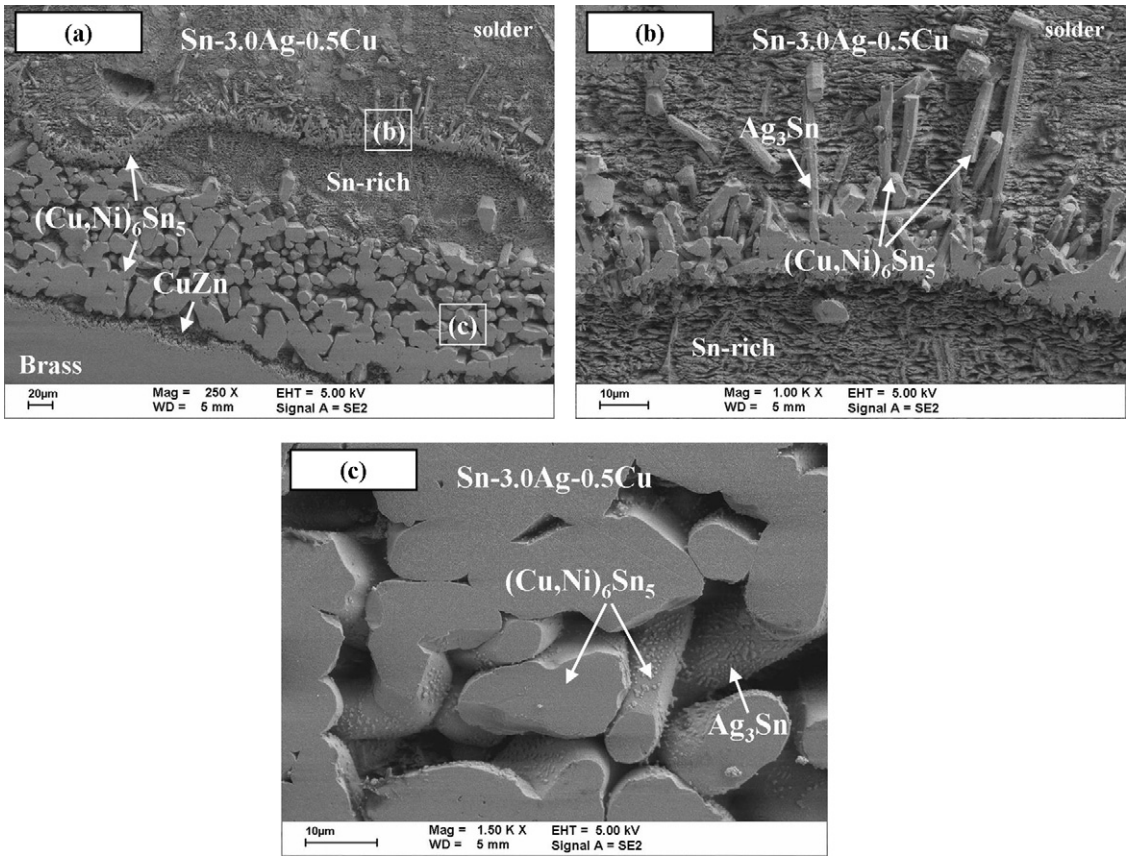

Fig. 4. (a) Deep-etched SEI micrograph of the SAC/Au/Pd/Ni/brass reaction system reacted at 270 °C for 8 h; (b) and (c) is magnified locally from (a).

(at.%), which is the CuZn phase [28]. The composition of the light gray, irregular and thick layer close to the SC side is Sn–27.2 Cu–24.0 Ni–1.9 Zn (at.%). This layer is the (Cu, Ni)$_6$Sn$_5$ phase [28]. When the reaction time was extended to 20 h, the CuZn and (Cu, Ni)$_6$Sn$_5$ phase were still formed at the interface and a significant grain ripening process in the (Cu, Ni)$_6$Sn$_5$ phase was found.

Fig. 5(a) shows an un-etched BEI micrograph of the SC/Au/Pd/Ni/brass couple at 270 °C for 8 h. Fig. 5(b) shows the SEI microstructure of the image presented in Fig. 5(a) after deep-etching. When the reaction time was extended the Ni atoms in the (Cu, Ni)$_6$Sn$_5$ phase were replaced by larger amount of Cu atoms from the SC solder and the brass substrate. The grain morphology of the (Cu, Ni)$_6$Sn$_5$ phase near the SC solder side was converted into a smoother column-type shape from the polyhedron-type. At the same time, the CuZn phase was formed at the interface. Similar to the Sn or SAC solders reacted with the Au/Pd/Ni/brass, there was no Cu$_3$Sn phase formed at the interface in the SC/Au/Pd/Ni/brass system.

The result and reaction mechanism in the SC/Au/Pd/Ni/brass were similar to that of the Sn or SAC reacted with the Au/Pd/Ni/brass substrate. These results are also similar to that found in the Cu content effect in SAC/Ni/Cu [16] and SC/Ni [29] couples. Related studies [16,30] indicated that only the (Cu, Ni)$_6$Sn$_5$ phase was formed at the solder/Ni/Cu or solder/Ni interface if the Cu content in the

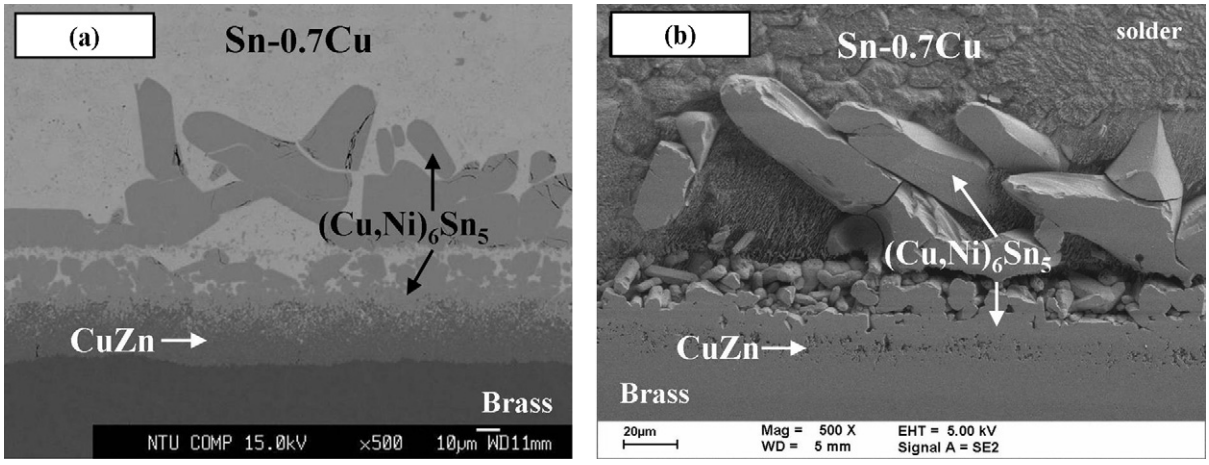

Fig. 5. (a) Un-etched BEI micrograph and (b) deep-etched SEI micrograph of the SC/Au/Pd/Ni/brass reaction couple reacted at 270 °C for 8 h.

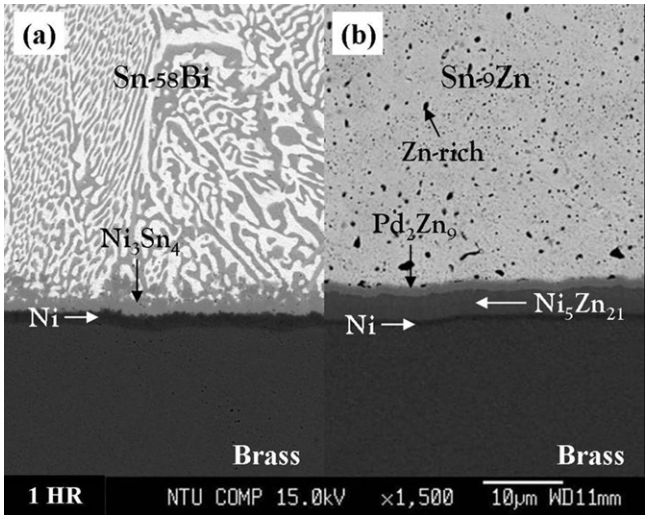

Fig. 6. BEI micrographs of the (a) SB/Au/Pd/Ni/brass and (b) SZ/Au/Pd/Ni/brass reaction systems reacted at 270 °C for 1 h.

solder was greater than 0.5 wt%. When the reaction temperature was reduced to 255 and 240 °C similar results were found. The IMC evolution is listed in Table 1.

3.4. Sn–58 Bi (SB)/Au/Pd/Ni/brass reaction couple

Fig. 6(a) shows a BEI micrograph of the SB/Au/Pd/Ni/brass system reacted at 270 °C for 1 h. The dark and light regions in the SB solder are typical Sn-rich and Bi-rich phase eutectic structures. A bright and planar layer close to the SB solder was found and its composition, determined by EMPA, was Sn–39.1 Ni–2.4 Cu–1.2 Pd–1.2 Zn (at.%). This layer should be the Ni_3Sn_4 phase [28]. The dark layer close to the brass side is the remnant Ni layer. Compared with the above systems no CuZn phase was formed at the interface. This result is very similar to the SB/Au/Pd/Ni/Cu system [14]. The Ni layer still acted as a diffusion barrier to prevent the Sn from reacting with the substrate. Only the Ni and Sn reacted with each other to form the Ni_3Sn_4 phase. The Ni layer was progressively consumed and remained at the interface when the reaction time was increased to 8 h, as shown in Fig. 7. At the brass side a non-continuous and broken Ni layer was observed. A few dark and non-continuous layers adhered to the brass could be found. This layer has a unique Cu–44.8 Zn–7.7 Sn–3.5 Ni–1.3 Pd (at.%) composition. It is considered to be

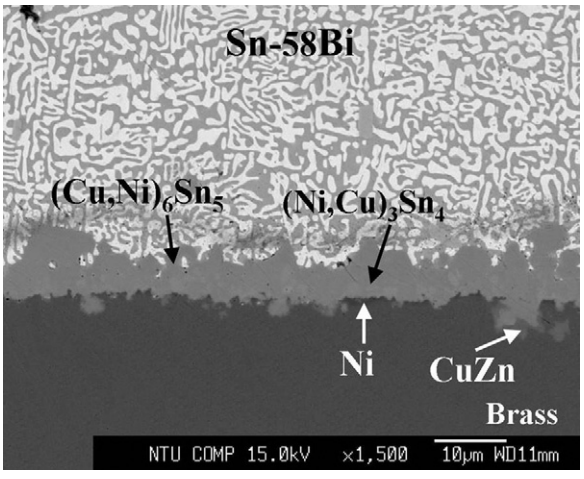

Fig. 7. BEI micrograph of the SB/Au/Pd/Ni/brass reaction system reacted at 270 °C for 8 h.

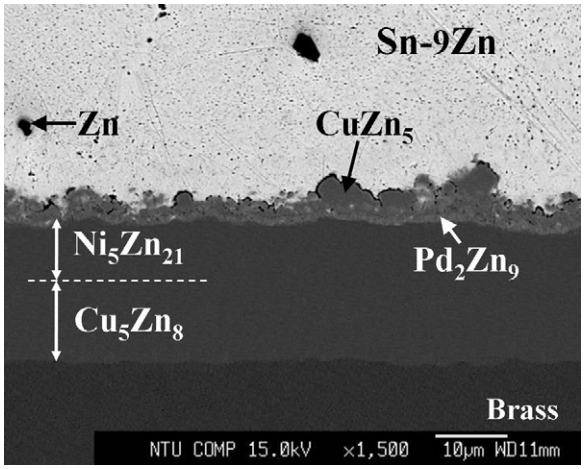

Fig. 8. BEI micrograph of the SZ/Au/Pd/Ni/brass reaction system reacted at 270 °C for 20 h.

the CuZn phase [26]. Thick and irregular regions with light-gray contrast and substantial thickness were formed close to the SB solder. The composition was Sn–27.8 Cu–22.9 Ni–3.4 Zn (at.%) and it was likely the $(Cu, Ni)_6Sn_5$ phase [28]. A third IMC, distributed randomly in the $(Cu, Ni)_6Sn_5$ phase near the substrate side was observed. It was the $(Ni, Cu)_3Sn_4$ phase of Sn–36.0 Ni–5.5 Cu–1.0 Zn (at.%) [28].

While the Ni layer gradually dissolved into the solder and reacted with the Sn to form the Ni_3Sn_4 phase, the non-continuous Ni remained at the interface and this Ni layer could not act as an effective diffusion barrier anymore. The large amount of Cu atoms from the brass substrate diffused toward the solder through the Ni_3Sn_4 phase to form the $(Cu, Ni)_6Sn_5$ phase close to solder and CuZn phase adhered to the brass side. When the reaction time was extended to 20 h, the Ni was consumed completely. Thus, the $(Ni, Cu)_3Sn_4$ phase was completely converted into the $(Cu, Ni)_6Sn_5$ phase and the reaction system changed from the SB/Au/Pd/Ni/brass system to the Sn/Au/Pd/Ni/brass. This reaction mechanism was similar to that of the Sn/Au/Pd/Ni/brass couples. Similar results were found when the reaction temperature was reduced to 255 and 240 °C. These results are listed in Table 1.

3.5. Sn–9 Zn (SZ)/Au/Pd/Ni/brass reaction couple

Fig. 6(b) shows the BEI image of the SZ/Au/Pd/Ni/brass system reacted at 270 °C for 1 h. A eutectic structure (Zn) phase with a black contrast and needle-like shape and β-Sn phase are observed in the SZ solder. The continuous planar layer near the brass side is the remaining Ni layer. Two continuous IMC layers were formed between the SZ solder and Ni. The smooth and light gray layer close to the SZ solder is the Pd_2Zn_9 phase of Zn–14.2 Pd–3.4 Cu–2.7 Ni (at.%) [28]. Another planar layer between the Pd_2Zn_9 phase and Ni layer had a unique Zn–16.3 Ni–1.9 Cu (at.%) composition and it was the Ni_5Zn_{21} phase [17,31]. The thin Au layer rapidly dissolved into the solder in the initial reaction [30], with high activity Zn atoms aggregated at the interface to easily react with electroplated elements of the substrate. Thus, the Pd_2Zn_9 phase was formed at the interface. Zn atoms continuously diffused toward the Ni layer and the Ni_5Zn_{21} phase was formed at the interface, as well. This result is very similar to the SZ/Au/Pd/Ni/Cu system [14].

When the reaction time was extended to 20 h, the Ni layer was completely consumed. Three different contrast layers are observed at the solder/brass interface, as shown in Fig. 8. The first layer with a scalloped shape, close to the SZ solder is composed of Zn–17.4 Cu–4.6 Pd–1.4 Sn (at.%). This layer should be the $CuZn_5$ phase

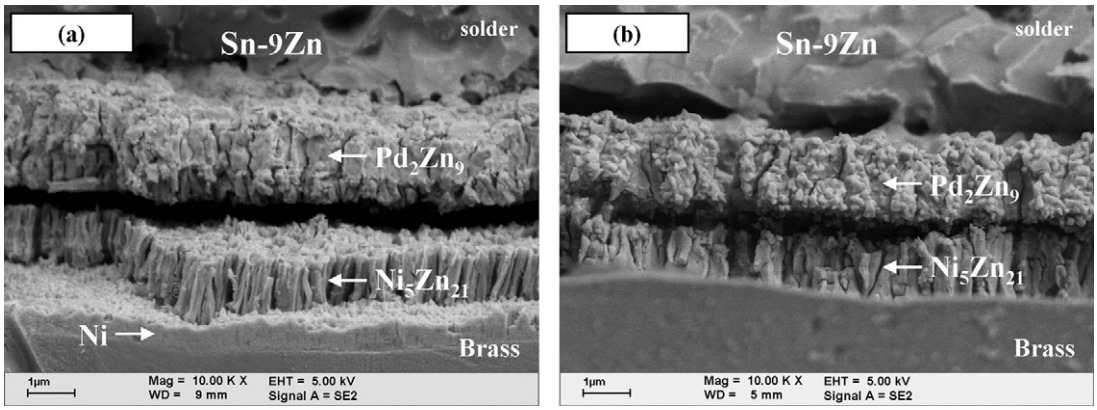

Fig. 9. Deep-etched SEI micrographs of the SZ/Au/Pd/Ni/brass reaction system reacted at 270 °C for (a) 1 h and (b) 8 h.

[14,26]. The second layer with a light-gray contrast is the Pd_2Zn_9 phase, composed of Zn–10.1 Pd–7.9 Cu–2.0 Sn–1.2 Ni (at.%) [14,28]. The third layer, close to the brass side has a unique Zn–14.9 Ni–1.8 Sn–1.2 Cu (at.%) composition, and it is likely the Ni_5Zn_{21} phase [14,28]. This result revealed that the Cu content in the Pd_2Zn_9 and Ni_5Zn_{21} phases at 20-h reaction time was greater than that for the 4-h reaction. The brass is the source of the Cu atoms in this reaction system. Since the Ni layer was consumed and destroyed, it could not act a diffusion barrier to block the Cu atoms from diffusing toward the SZ solder. The Cu, Zn and Ni diffusion rates in the liquid Sn were Cu > Zn > Ni > Sn [32]. Therefore, the Cu and Zn atoms from the brass rapidly diffused through the Pd_2Zn_9 and Ni_5Zn_{21} phases to the interface and reacted with the Zn atoms from the SZ solder to form the $CuZn_5$ phase, which was the Cu-rich Zn IMC. The Cu dissolved into the Pd_2Zn_9 and Ni_5Zn_{21} phases due to the considerable solubility between Cu–Pd and Cu–Ni systems [28]. When a great amount of Cu atoms diffused toward the SZ solder, the Zn concentration in the Ni_5Zn_{21} phase/brass interface became high. The Zn atoms could continue to react with the remaining Cu atoms to form the $CuZn_5$ phase, which was a stable Cu-rich Zn IMC. The brass substrate has 40 wt% Zn in it. Both Zn from the SZ solder and brass diffused toward the Ni layer. Thus, the diffusion flux of the Zn increased from both sides and reacted with the Ni layer to form the Ni_5Zn_{21} phase, not the NiZn phase. That's why the Ni-rich Zn IMC was formed at the interface.

Fig. 9(a) and (b) show deep-etched SEI micrographs of the SZ/Au/Pd/Ni/brass couples reacted at 270 °C for 1 h and 8 h, respectively. Two planar layer IMC phases can be observed in Fig. 9. The above IMC layer near the SZ solder is the Pd_2Zn_9 phase and the other layer is the Ni_5Zn_{21} phase. In this system, no cracks were found in the Ni_5Zn_{21} phase. However, there were many cracks in the Ni_5Zn_{21} phase in the SZ/Au/Pd/Ni/Cu system [14]. In the SZ/Au/Pd/Ni/Cu system, the NiZn phase was form in the early stage. When the reaction time was increased, the NiZn phase was transformed to the Ni_5Zn_{21} phase. This crack might be due to the phase transformation. However, only the Ni_5Zn_{21} phase was formed in the SZ/Au/Pd/Ni/brass system and no phase transformation occurred between the Ni–Zn IMCs. Therefore, no cracks were found in this reaction system. The IMC evolution in the SZ/Au/Pd/Ni/brass systems reacted at 250 and 240 °C are listed in Table 1.

4. Conclusions

The interfacial reactions of Sn, Sn–3.0 wt% Ag–0.5 wt% Cu (SAC), Sn–0.7 wt% Cu (SC), Sn–58 wt% Bi (SB) and Sn–9 wt% Zn (SZ) lead-free solders with Au/Pd/Ni/brass multilayer substrate were systematically investigated in this study. The detailed IMC evolution for each system was obtained. The results revealed that the major IMCs formed at the interface were the $(Cu, Ni)_6Sn_5$ and CuZn phases in the Sn, SAC, and SC solders reacted with the Au/Pd/Ni/brass. The $(Ni, Cu)_3Sn_4$, $(Cu, Ni)_6Sn_5$ and CuZn phases were formed in the SB/Au/Pd/Ni/brass system. The $CuZn_5$, Pd_2Zn_9, Ni_5Zn_{21} and Cu_5Zn_8 were formed between the SZ solder and Au/Pd/Ni/brass substrate. Because the brass contained 40 wt% Zn in it and Cu atoms from the brass diffused toward the solder, the Cu–Zn IMCs were formed in all reaction couples. This Cu–Zn IMCs acted as a diffusion barrier. Thus, the Cu_3Sn phase was not formed at the interface. Our current study results reveal that the IMC formation in the solder/Au/Pd/Ni/brass systems is very sensitive to the reaction times. Therefore, the electronic industry must assess their choice of optimal reflowing and aging conditions to ensure the joints exhibit consistent interfacial properties. This information is very valuable for the soldering community.

Acknowledgements

The authors acknowledge the financial support of the National Science Council of Taiwan, Republic of China (Grant nos. NSC 99-2628-E-011-009 and 100-2628-E-011-003) and are grateful to Mr. C.Y. Kao for carrying out the EPMA analysis and Mr. Laiw for carrying out the FE-SEM analysis.

References

[1] J.W. Yoon, S.B. Jung, J. Alloys Compd. 396 (2005) 122–127.
[2] C.P. Lin, C.M. Chen, Y.W. Yen, H.J. Wu, S.W. Che, J. Alloys Compd. 509 (2011) 3509–3514.
[3] D.M. Settle, C.C. Patterson, Science 207 (1980) 1167–1176.
[4] Official Journal of the European Union 13.2 (2003) L37/19–L37/23.
[5] S.W. Chen, Y.W. Yen, J. Electron. Mater. 28 (1999) 1203–1208.
[6] A. Sharif, Y.C. Chan, J. Alloys Compd. 390 (2005) 67–73.
[7] R.M. Shalaby, J. Alloys Compd. 505 (2010) 113–117.
[8] A.A. El-Daly, A.E. Hammad, J. Alloys Compd. 505 (2010) 793–800.
[9] A.A. El-Daly, F. El-Tantawy, A.E. Hammad, M.S. Gaafar, E.H. El-Mossalamy, A.A. Al-Ghamdi, J. Alloys Compd. 509 (2011) 7238–7246.
[10] Y.W. Yen, Y.C. Chiang, C.C. Jao, D.W. Liaw, S.C. Lo, C. Lee, J. Alloys Compd. 509 (2011) 4595–4602.
[11] M. Yang, M. Li, L. Wang, Y. Fu, J. Kim, L. Weng, Mater. Lett. 65 (2011) 156–1509.
[12] L.C. Tsao, C.O. Chu, S.F. Peng, Microelectron. Eng. 88 (2011) 2964–2969.
[13] Y.W. Yen, W.T. Chou, Y. Tseng, C. Lee, C.L. Hsu, J. Electron. Mater. 37 (2008) 73–83.
[14] Y.W. Yen, P.H. Tsai, Y.K. Fang, S.C. Lo, Y.P. Hsieh, C. Lee, J. Alloys Compd. 503 (2010) 25–30.
[15] C.E. Ho, L.C. Shiau, C.R. Kao, J. Electron. Mater. 31 (2002) 1264–1269.
[16] C.E. Ho, R.Y. Tsai, Y.L. Lin, C.R. Kao, J. Electron. Mater. 31 (2002) 584–590.
[17] F. Zhang, M. Li, C.C. Chum, Z.C. Shao, J. Electron. Mater. 32 (2003) 123–130.
[18] C.E. Ho, S.C. Yang, C.R. Kao, J. Mater. Sci.: Mater. Electron. 18 (2006) 155–174.
[19] Y.W. Yen, W.K. Liou, J. Mater. Res. 22 (2007) 2663–2667.
[20] Y.W. Yen, C.Y. Lee, M.H. Kuo, K.S. Chao, K.D. Chen, Int. J. Mater. Res. 100 (2009) 672–676.

[21] Y.W. Yen, W.T. Chou, H.C. Chen, W.K. Liou, C. Lee, Int. J. Mater. Res. 99 (2008) 1256–1261.
[22] S.K. Lin, K.D. Chen, H. Chen, W.K. Liou, Y.W. Yen, J. Mater. Res. 25 (2010) 2278–2286.
[23] Y.W. Yen, D.W. Liaw, K.D. Chen, H. Chen, J. Electron. Mater. 29 (2010) 2412–2417.
[24] C.F. Tseng, T.K. Lee, G. Ramakrishna, K.C. Liu, J.G. Duh, Mater. Lett. 65 (2011) 3216–3218.
[25] A. Kumar, Z. Chen, J. Electron. Mater. 40 (2011) 213–223.
[26] K.S. Kim, J.M. Yang, C.H. Yu, I.O. Jung, H.H. Kim, J. Alloys Compd. 379 (2004) 314–318.
[27] P. Harris, Solder. Surf. Mount Technol. 1/3 (1999) 46–52.
[28] H. Baker (Ed.), ASM Handbook-Alloy Phase Diagram, vol. 3, ASM International, Materials Park, OH, 1992, 2.178, 2.182, 2.318, 2.321, 2.344.
[29] D.P. He, D.Q. Yu, L. Wang, C.M.L. Wu, Chin. J. Nonferr. Met. 16 (2006) 701–708.
[30] C.E. Ho, Y.M. Chen, C.R. Kao, J. Electron. Mater. 28 (1999) 1231–1237.
[31] C.Y. Chou, S.W. Chen, Y.S. Chang, J. Mater. Res. 21 (2006) 1849–1856.
[32] B.F. Dyson, T.R. Anthony, D. Turnbull, J. Appl. Phys. 38 (1967) 3408.